Wide Dynamic Range Sensing in Photonic Crystal Microcavity Biosensors

Chun-Ju Yang[1]*, Hai Yan[1],Yi Zou[1], Swapnajit Chakravarty[2]*, Naimei Tang[2], Zheng Wang[1], Ray T. Chen[1],[2]*

[1]Dept. Electrical and Computer Engineering, The University of Texas at Austin, 10100 Burnet Rd, PRC/MER 160, Austin, Tx78758, USA [2]Omega Optics, Inc., 10306 Sausalito Dr, Austin, TX78759, USA

chunjuyang@utexas.edu, swapnajit.chakravarty@omegaoptics.com, ray.chen@omegaoptics.com, Fax: +1-512-471-8575

Abstract: Typical L-type photonic crystal (PC) microcavities have a dynamic range of approximately 3-4 orders of magnitude in biosensing. We experimentally demonstrated that multiplexing of PC sensors with different geometry can achieve a wide dynamic range covering 6 orders of magnitude.

In several applications of biosensing, such as drug discovery and therapeutic drug monitoring, it is essential to have sensors that can register concentrations of analytes over a wide dynamic range of at least five orders of magnitude [1]. Recently, numerous optical devices have been investigated for label free detections, such as ring resonators [2], surface plasmon resonance (SPR) [3], wire waveguides [4], and photonic crystal (PC) microcavities [5]. Among all the label free optical devices, photonic crystal (PC) waveguides have provided the unique characteristics with slow light effect which enhances the interaction between traveling light the analyte. The slow light effect in PC sensors has been investigated by our group in numerous applications such as near-IR absorption chemical and bio-sensing [6], gaseous contaminant detection [7], and two-dimensional PC biosensors for chip-integrated microarray applications in proteomics [8]. However, each PC microcavity sensor we have demonstrated including L3, L13 and L55 where Ln represents that the PC microcavity is formed by removing n air holes in a row along the Γ-K direction, the PC cavity being located next to a W1 photonic crystal waveguide (PCW), have a dynamic range of approximately 4 orders of magnitude, with the linear region of the concentration versus wavelength shift curve being linear over just 3 orders of magnitude. Integrated optics however provides the unique ability to multiplex sensors on the same chip that can be measured simultaneously at the same time with the same sample due to the miniaturized dimensions of the sensors. In this paper, we experimentally demonstrate a novel design for achieving wide dynamic detection range whereby multimode interference (MMI) devices are integrated with photonic crystal microcavities of different geometries, each covering a different concentration range and thereby achieving a wide dynamic range of 6 orders of magnitude.

We fabricated PCWs on silicon-on-insulator (SOI) devices with a 250nm top silicon layer, a 3μm buried oxide layer. Fig. 1 shows a scanning electron micrograph (SEM) of the individual PC sensors. Four distinct sensors with four different

Optical Fibers and Sensors for Medical Diagnostics and Treatment Applications XV, edited by Israel Gannot
Proc. of SPIE Vol. 9317, 931713 · © 2015 SPIE · CCC code: 1605-7422/15/$18
doi: 10.1117/12.2080645

geometries, L3, L13H, L55 and L21 are fabricated where L13H denotes that defect holes that are smaller in size than the radius of the holes in the bulk PC lattice are integrated. The four discrete PC microcavities are fanned out on the 4 arms of a 1×4 MMI [5, 9]. The respective SEMs are shown in Figs. 1(a)-(e). With L3, L55 and L21, the adjacent coupling PCW is of the W1 which indicates that the width of PCW is$\sqrt{3}a$, where a is the lattice constant. For L13H, the width of the coupling PCW is $0.935\sqrt{3}a$. The PC consists of a triangular lattice of air holes with lattice constant a=392.5 nm. The air holes have radius r=0.277a. The air hole diameter is d=0.53a, and silicon slab thickness is h=0.63a. The diameter of defect holes in L13H is 0.4d and thus indicated as L13H0.4 in Fig. 1.

A typical transmission spectrum of the four different PCWs with PC microcavities of different geometry coupled to the PCW in water is shown in Fig 2(a)-(d). The sensor works on the principle that refractive index changes in the vicinity of the PC microcavities lead to a shift in the resonance wavelength, the sensitivity of the sensor determined by the magnitude of the resonance wavelength change for a given change in refractive index in chemical sensing, or a given change in biomolecule concentration in biosensing. Bio sensing experiments were conducted by selecting biotin as the probe immobilized to the patterned silicon substrate and avidin as target protein. In contrast to our previous demonstrations in lung cancer cell line lysate detection where each PC microcavity on the four arms of the MMI were of the same geometry and were immobilized with different probes to show both sensing and specificity of detection [9], in this paper, all the four PC microcavities on the 4 arms were immobilized with the same probe.

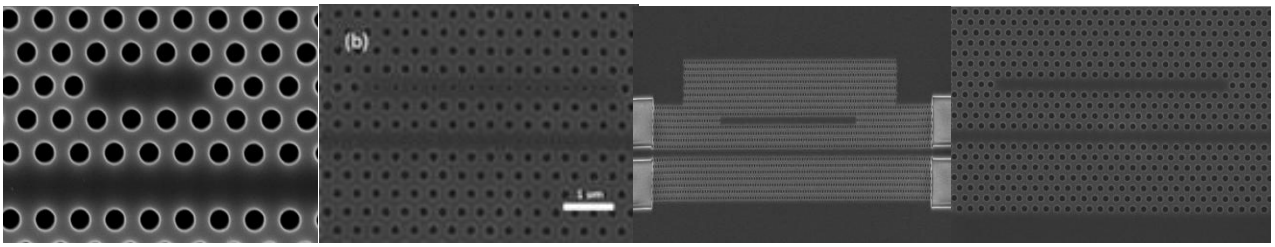

(a) (b) (c) (d)

(e)

Fig 1. SEM image of PC microcavities coupled to PCW in (a) L3 (b)L13H0.4 defect hole cavity (c) L55and (d) L21 PC microcavities (e) Microscopic image of the MMI coupler and four PC sensors on the four channels.

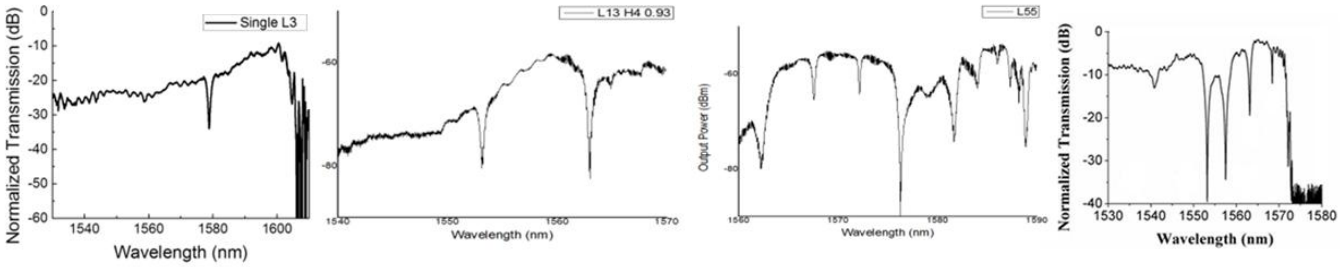

Fig 2. Transmission spectrum of (a) L3 (b) L13H0.4 defect hole cavity (c) L55and (d) L21 PC microcavities

The measurement setup is shown in Fig 3. Input TE polarized light is coupled to the input subwavelength (SWG) grating with a polarization maintaining single mode fiber. Light is coupled out of the output SWG via a standard single mode fiber. Light is guided in and out of the photonic crystal waveguide (PCW) by ridge waveguide with PC group index taper to enable high coupling efficiency into the slow light guided mode. The PCW adiabatic group index taper, shown in Fig. 3(c), is achieved by gradually increasing the widths of the first eight periods of PCW to reduce the group index.

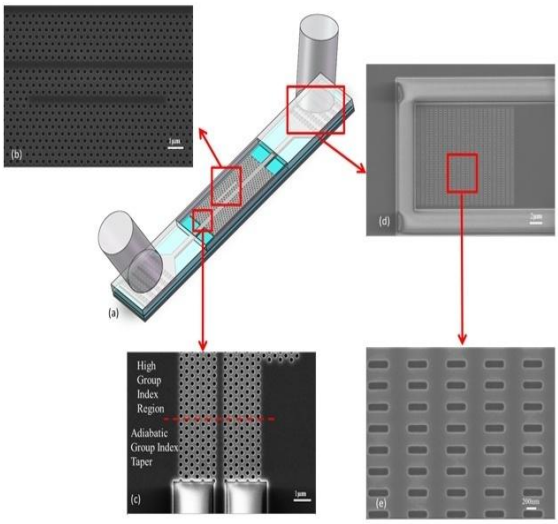

Fig. 3. (a) Schematic of the whole device, (b) close up of the L21 PC microcavity (c) SEM picture of the fabricated PCW device showing the PCW adiabatic group index taper achieved by adiabatic width taper of PCW and high group index region, (d) SEM image of fabricated grating coupler, and (e) magnified view of air holes

The chip was treated chemically and the probe protein (Biotin) was immobilized on the surface. Before target test, 1% bovine serum albumin (BSA) was used to block any binding sites that have not been covered by probe proteins. After a thorough wash in phosphate buffered saline (PBS), the device was ready for test. Before applying any target solution, resonance spectrum for each device was recorded and the resonance position was used as baseline. The chip is then incubated in target solution for 40 min. Several concentrations of the target were measured. After each incubation, the chip was washed with PBS and new spectra were tested and resonance positions were further recorded.

The resonance shift as a function of concentration was measured for each individual PC microcavity, as shown in Fig. 4.

The dashed red line indicates the minimum detection limit for each PC microcavity, limited by the wavelength resolution of our optical spectral analyzer of +/- 0.02nm. The different detection ranges of the four types of PC sensors can be identified. Below 10^{-13} M, only the most sensitive device, L13 with defect holes, shows resonance shift over noise level. From 10^{-13}M to 10^{-12} M, L55 shows shifts from 0.04 nm to 0.3 nm indicating the biomolecule binding has been detected. The detection range of L21 is between 10^{-12}M and 10^{-10}M. L3 starts to detect effectively after reaching 10^{-11}M. This is also the range of concentrations within which the resonance shift is linearly proportional to the log of the concentration, as depicted in Fig. 4, the detection range corresponding to each individual device is marked in dashed blue line. Beyond each of the ranges, the shift gradually reaches an upper limit when the target captured at the PC sensor saturates the effective sensing area. The detection range is from 10^{-15} M to 10^{-9} M was achieved by combining the individual ranges from the different PC microcavities.

In summary, six orders of magnitude wide dynamic range detection, from 10^{-15} M to 10^{-9} M was demonstrated using PC sensors of different sensitivities multiplexed by a MMI power splitter. The multiplexed wide detection range chip holds significant promise application in biosensing monitoring.

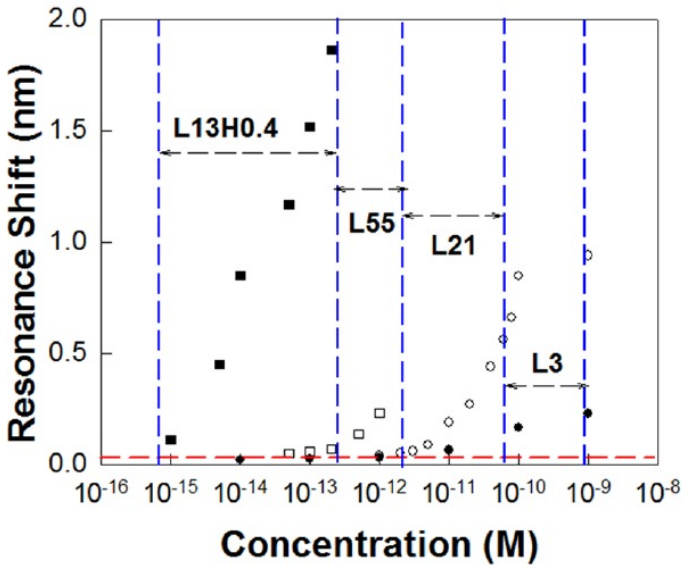

Fig. 4. Biosensing spectral shifts in L13, L21, L55 and L13 defect holed cavity.

References

[1] MG. Scullion, A. Di Falco, TF. Krauss Biosens Bioelectron, 27:101–5 (2011)

[2] M. Iqbal, M. A. Gleeson, B. Spaugh, F. Tybor, W. G. Gunn, M. Hochberg, T. Baehr-Jones, R. C. Bailey, and L. C. Gunn, IEEE J. Sel. Top. Quantum Electron.16, 654 (2010).

[3] H. Sipova, S. Zhang, A. M. Dudley, D. Galas, K. Wang, and J. Homola, Anal. Chem. 82, 10110 (2010).

[4] A. Densmore, M. Vachon, D. X. Xu, S. Janz, R. Ma, Y. H. Li, G. Lopinski, A. Delage, J. Lapointe, C. C. Luebbert, Q. Y. Liu, P. Cheben, and J. H.

Schmid, Opt. Lett. 34, 3598 (2009).

[5] Y. Zou, S. Chakravarty, W.-C. Lai, C.-Y. Lin and R. T. Chen, Lab Chip, 2012, 12, 2309–2312.

[6] W. Lai, S. Chakravarty, Y. Zou, and R. T. Chen, Opt. Lett. 37, 1208–1210 (2012).

[7] W.-C. Lai, S. Chakravarty, X. Wang, C. Lin, and R. T. Chen, Optics Letters 36, 984–6 (2011)

[8] S. Chakravarty, Y. Zou, W.-C. Lai, and R.T. Chen, Biosensors & Bioelectronics 38, 170 (2012)

[9] S. Chakravarty, W-C. Lai, Y. Zou, H.A. Drabkin, G.R. Simon, S.H. Chin, R. M. Gemmill, R.T. Chen, Biosens. Bioelectron. 43, 50 (2013).

[10] X. Xu, H. Subbaraman, J. Covey, D. Kwong, A. Hosseini, and R. T. Chen, Appl. Phys. Lett., vol. 101, pp. 31109-1–031109-3, (2012).